ELSEVIER

Journal of Fluids and Structures 25 (2009) 629–640

JOURNAL OF FLUIDS AND STRUCTURES

www.elsevier.com/locate/jfs

The interaction of a gravity current with a circular cylinder mounted above a wall: Effect of the gap size

E. Gonzalez-Juez[a], E. Meiburg[a,*], G. Constantinescu[b]

[a]*Department of Mechanical Engineering, University of California at Santa Barbara, CA 93106-5070, USA*
[b]*Department of Civil and Environmental Engineering, University of Iowa, USA*

Received 3 April 2008; accepted 20 January 2009
Available online 18 March 2009

Abstract

The flow of a gravity current past a circular cylinder mounted above a bottom wall is studied by means of two-dimensional Navier–Stokes simulations. The investigation focuses on the effects of the gap size on the forces acting on the cylinder. The interaction of the current with the cylinder can be divided into an impact, a transient, and a quasisteady stage. During the impact stage, the gravity current meets the cylinder, and the drag increases towards a maximum, while the lift undergoes a drastic fluctuation which increases noticeably with the gap size. During the quasisteady stage, the flow past the cylinder resembles that observed in constant-density boundary layer flows past cylinders: Karman vortex shedding is observed for sufficiently large gap sizes, while a vorticity cancellation mechanism is responsible for the suppression of vortex shedding at small gap sizes. On the other hand, interesting differences that distinguish the gravity current case from the constant-density case are the presence in the gravity current flow of a component of the mean quasisteady lift due to buoyancy, and another component from the deflection of the wake towards the wall by the constriction of the dense fluid flow downstream of the cylinder, as well as the cancellation of vortex shedding for all gap sizes when the ratio of the channel depth to lock height is decreased from 5 to 1.

Keywords: Flow–structure interaction; Vortex shedding; Gravity current; Circular cylinder; Numerical simulation

1. Introduction

Gravity currents form in natural environments and engineering applications when a heavier fluid propagates into a lighter one in a predominantly horizontal direction (Simpson, 1997; Benjamin, 1968). In the ocean, such currents can reach heights of up to $O(100\,\mathrm{m})$ and velocities in the range of $O(1\text{–}10\,\mathrm{m/s})$ (Kneller et al., 1999), so that they pose a serious hazard to submarine installations. Consequently, several recent investigations have focused on the unsteady loads caused by gravity currents impinging on submerged structures (Ermanyuk and Gavrilov, 2005a, b; Gonzalez-Juez et al., 2007, 2008). The dominant physical mechanisms are of fundamental interest, due to the transient nature of the interaction between the propagating front and the stationary object. Such transient interactions have not received much attention in the past, as most flow–structure investigations have addressed the problem of uniform flow past cylinders [cf. the review by Williamson (1996)].

*Corresponding author.
E-mail address: meiburg@engineering.ucsb.edu (E. Meiburg).

0889-9746/$ - see front matter © 2009 Elsevier Ltd. All rights reserved.
doi:10.1016/j.jfluidstructs.2009.01.002

Recent experimental investigations have measured time-varying drag and lift of gravity current flows over circular and square cylinders mounted above a wall (Ermanyuk and Gavrilov, 2005a, b). However, as the experimental methods employed do not provide a detailed description of the flow field, they cannot establish a link between transient forces and specific flow structures. In this regard, numerical simulations have been able to provide additional relevant information (Gonzalez-Juez et al., 2007, 2008). The gravity current flow past a bottom-mounted square cylinder is considered in Gonzalez-Juez et al. (2008). This work identifies, through a parametric study, the dominant flow parameters and the proper scaling of the force magnitude and frequency, emphasizing the description of the mechanisms that generate the drag. The maximum drag is seen to occur when the gravity current meets the cylinder. An upper bound is given for this maximum drag. Three-dimensional simulations show that the impact is, essentially, of two-dimensional nature. Later on, the flow-field around the cylinder reaches a quasisteady state. During this stage, an interesting difference with the constant-density flow past a bottom-mounted square cylinder is the presence of a hydrostatic component of the drag.

Submarine pipelines represent an important class of structures at risk by gravity currents. The largest force fluctuations experienced by such pipelines are known to occur along sections where the pipeline is separated from the ocean floor by a gap, as a result of scouring. Early attempts to model this situation considered constant-density boundary layer flows past circular cylinders above a non-erodible bottom wall (Bearman and Zdravkovich, 1978; Zdravkovich, 1985; Lei et al., 1999, 2000). These studies showed that the gap between the cylinder and the bottom has an important effect on the unsteady force. For sufficiently large gap sizes, force fluctuations were found to be caused primarily by vortex shedding. Hence lift fluctuations are usually larger than drag fluctuations. However, the constant-density boundary layer flows employed in the above investigations are known to differ from gravity currents in important ways. This represents the main motivation for the current investigation, which considers the flow of a lock-exchange Boussinesq gravity current past a circular cylinder near a non-erodible bottom wall. The objective of the present work is to explain the physical mechanisms that generate the force on the cylinder, by studying the effect of the gap size, the ratio of the channel depth and the lock-height, and of the Reynolds number on this force, using detailed information of the flow field given by two-dimensional numerical simulations. In contrast to gravity currents flowing past a bottom-mounted square cylinder (Gonzalez-Juez et al., 2008), the flow of a gravity current past a cylinder mounted a distance *above* the wall should exhibit richer and more interesting dynamics, and is of more practical relevance. Lift fluctuations are now more important, so that we will explore them in detail. Furthermore, the gravity current flow of a cylinder cannot be analyzed in a straightforward fashion on the basis of the shallow water equations (Rottman et al., 1985; Lane-Serff et al., 1995; Gonzalez-Juez et al., 2009).

Two-dimensional simulations are able to capture many details of the gravity current front, such as its speed and height during the constant front speed regime (Härtel et al., 2000a; Ooi et al., 2005), although a spanwise structure is known to form in three-dimensional gravity currents (Simpson, 1997; Härtel et al., 2000a, b). Similarly, two-dimensional bluff body flow simulations reproduce most of the dominant flow structures, although at higher Reynolds numbers pronounced spanwise features exist (Williamson, 1996; Mittal and Balachandar, 1995). On the other hand, the proximity to a wall reduces some of these three-dimensional effects (Bailey et al., 2002). Recently, it has been found that at high Reynolds numbers two-dimensional simulations of gravity currents flows past square cylinders can predict unphysical forces fluctuations (Gonzalez-Juez et al., 2008). Therefore, the present investigation focuses on rather low Reynolds numbers, at which two-dimensional simulations would not be severely "contaminated" with three-dimensional effects. The dominant physical mechanisms at work are expected to be revealed by these simulations. However, a subsequent extension of the present work to three-dimensional high-Reynolds number flows is desirable.

The manuscript is organized as follows. Section 2 defines the geometrical set-up of the problem, the set of governing equations, and the governing parameters. The parameter range of the simulations is discussed in Section 3.1. Section 3.2 describes the temporal evolution of the flow field for a reference case. The important effect of the gap size on the unsteady force is discussed in Section 3.3. The results are divided into the impact, transient, and quasisteady stages of the interaction. The effect of the channel depth is discussed in Section 3.4. Section 3.5 discusses the effect of the Reynolds number, with an emphasis on the lift fluctuations. Finally, Section 4 summarizes the main findings and conclusions.

2. Problem description and computational approach

Fig. 1 shows a sketch of the channel of length L and height H, filled with ambient fluid of density ρ_0. Submerged in it is a lock of length l and height h, which contains the denser fluid of density ρ_1. The difference in density between the fluids is assumed to be produced by different concentrations of a solute. This concentration is c_0 in the ambient fluid,

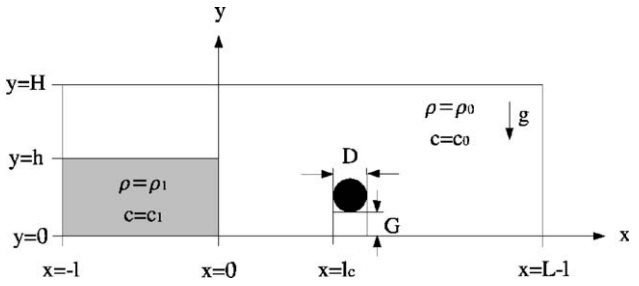

Fig. 1. Schematic of the flow configuration. A channel of length L and height H contains a lock of length l and height h. When the gate at $x = 0$ is opened, a current of the denser fluid forms and propagates towards a circular cylinder of diameter D, which is situated a distance l_c away from the gate, and a distance G above the bottom wall.

and c_1 in the fluid inside the lock. When the vertical gate at $x = 0$ is opened, a current of the denser fluid forms and propagates towards the right along the floor of the channel. After travelling a distance l_c, it encounters a circular cylinder of diameter D, placed a distance G above the bottom wall.

The simulations are based on the two-dimensional Navier–Stokes equations in the Boussinesq approximation (Härtel et al., 2000a; Ooi et al., 2005; and others). The buoyancy velocity is given by $u_b = \sqrt{g'h}$, where the reduced gravity g' is defined as $g' = g(\rho_1 - \rho_0)/\rho_0$. The relationship between density and concentration c is assumed to be linear, and given by $\rho = \rho_0 + (\rho_1 - \rho_0)(c - c_0)/(c_1 - c_0)$. By using u_b as the velocity scale, and h as the length scale, which results in a time scale of h/u_b, the following dimensionless variables, denoted with asterisks, are defined: $\mathbf{u}^* = \mathbf{u}/u_b$, $p^* = (p - p_{\text{ref}})/(\rho_0 u_b^2)$, and $c^* = (c - c_0)/(c_1 - c_0)$. Here, $\mathbf{u}$ denotes the velocity vector, p the total pressure, and p_{ref} a reference pressure. With such nondimensionalization, the conservation of mass, momentum, and concentration take the form

$$\boldsymbol{\nabla} \cdot \mathbf{u}^* = 0, \tag{1}$$

$$\frac{\partial \mathbf{u}^*}{\partial t^*} + \boldsymbol{\nabla} \cdot \mathbf{u}^* \mathbf{u}^* = -\boldsymbol{\nabla} p^* + \frac{1}{\text{Re}} \nabla^2 \mathbf{u}^* + c^* \mathbf{e}^g, \tag{2}$$

$$\frac{\partial c^*}{\partial t^*} + \boldsymbol{\nabla} \cdot c^* \mathbf{u}^* = \frac{1}{\text{Re}\,\text{Sc}} \nabla^2 c^*, \tag{3}$$

where $\mathbf{e}^g$ indicates the unit vector pointing in the direction of gravity. Eq. (3) expresses how the solute is redistributed throughout the flow field through the processes of convection and Fickian diffusion, and indicates that this solute is neither created nor destroy by chemical reactions.

The dimensionless governing parameters are the Reynolds number $\text{Re} = u_b h/\nu$ and the Schmidt number $\text{Sc} = \nu/\kappa$, where ν represents the kinematic viscosity and κ the molecular diffusivity, respectively. A Reynolds number based on the cylinder diameter D and the gravity current front speed V (to be defined later) is also used throughout the present work, and is given by $\text{Re}_D = VD/\nu$. In addition, there are various geometrical parameters, the most important ones being H/h, D/h, and G/h.

The bottom ($y = 0$) and left ($x = -l$) boundaries of the computational domain, and the surface of the cylinder, are treated as no-slip walls. The top boundary ($y = H$) is considered to be a slip wall, so that the wall-normal velocity is zero, along with the wall-normal derivative of the tangential velocity. A convective boundary condition is employed along the right boundary ($x = L - l$) of the domain (Pierce, 2001). The flow field is initialized with the fluid at rest everywhere, with a dimensionless concentration c^* of one inside the lock, cf. Fig. 1, and zero outside the lock.

A well-validated finite-volume code is used in this work (Pierce, 2001; Pierce and Moin, 2004; Gonzalez-Juez et al., 2008). The momentum and concentration conservation equations are discretized on a nonuniform Cartesian mesh, which is refined close to the no-slip walls. Time integration is accomplished via an iterative procedure similar to the Crank–Nicolson scheme. To ensure that the continuity equation is satisfied, a Poisson equation for the pressure correction is solved at each time step. The simulation of irregular domains is accomplished by means of a grid blanking methodology. The converged results obtained with this code for the mean drag, rms-fluctuations of the lift, and the Strouhal number for the classic problem of a constant-density flow past a circular cylinder were found to be within 6% of those reported by Mittal and Balachandar (1995) at $\text{Re}_D = 525$. Furthermore, preliminary results obtained with this code closely reproduce the experiments by Ermanyuk and Gavrilov (2005a), cf. Gonzalez-Juez et al. (2007).

3. Results and analysis

3.1. Parameter range of the simulations

Table 1 indicates the parameter ranges of the simulations. The computational domain length is kept at $L/h = 24$ for all simulations. The constant lock length of $l/h = 9$ ensures that reflections from the left wall do not influence the interaction between the gravity current front and the structure, during the time of the simulation. The distance between the gate and the structure is chosen as $l_c/h = 3$, so that the current is in the constant front speed phase when it encounters the structure (Simpson, 1997; p. 167). We focus on results for the ratio of the channel height and the lock height $H/h = 5$, which approximates the deep ambient case of $H/h \to \infty$ found in practice (Gonzalez-Juez et al., 2008). We will discuss results for Reynolds numbers of $\mathrm{Re} = 2000$ ($\mathrm{Re}_D = 177$) and 6000 (558), which are representative for laboratory gravity currents [e.g. Ermanyuk and Gavrilov (2005a, b)]. A transition to three-dimensionality is known to exist in the range $\mathrm{Re}_D = 194-260$ in constant-density flows past circular cylinders (Williamson, 1996). Thus, the present investigation focuses on results for $\mathrm{Re}_D = 177$, at which two-dimensional simulations fully capture the dynamics of the flow near the cylinder. Even though the simulations for $\mathrm{Re}_D = 558$ do not capture the three-dimensional flow structures in the cylinder wake, we expect the results from these simulations not to be severely contaminated, as assumed by Lei et al. (2000), since the dominant physical mechanisms are of two-dimensional nature. The results for $\mathrm{Re}_D = 558$ are very useful, however, when compared to results from *two-dimensional* simulations of constant-density flows past circular cylinders near walls, as discussed later in Section 3.5. The Schmidt number Sc is kept at unity. The cylinder diameter is set to $D/h = 0.15$ in the present work. For comparison, typical gravity current heights of $O(1–100\,\mathrm{m})$ and cylinder length scales of $O(1\,\mathrm{m})$ yield a range of $D/h = 0.005-0.5$. We explore a range of gap widths $G/D = 0.067–1.33$ ($G/h = 0.01–0.2$), which corresponds to values typically generated through scouring [e.g.Sumer and Fredsoe (1990); Liang and Cheng (2005)]. A grid of 3000×400 is employed, along with a time step of $\Delta t/(h/u_b) = 0.0008$. The grid spacing near the cylinder is $0.015D$.

3.2. Reference case: description of the flowfield

Fig. 2 displays the temporal evolution of the vorticity field ($\omega/(V/h)$) as the gravity current interacts with the cylinder for $\mathrm{Re} = 2000$, $H/h = 5$, and $G/h = 0.15$. The miscible interface between the two fluids can be identified as a layer of positive vorticity in Fig. 2. An impact, a transient, and a quasisteady stage can be distinguished (Ermanyuk and Gavrilov, 2005a, b). Initially, the current approaches the cylinder from the left with a constant front speed of $V/u_b = 0.59$ (0.62) for $\mathrm{Re} = 2000$ ($\mathrm{Re} = 6000$). This front speed was calculated by tracking the foremost point of the $c^* = 0.5$ concentration isoline. The thickness of the gravity current is approximately $h/2$ (Shin et al., 2004). Fig. 2(a) shows the familiar structure of the head of the gravity current (Simpson, 1997; Härtel et al., 2000a; and others), as well as Kelvin–Helmholtz type vortices at the interface that separates the current from the ambient fluid. When encountering the cylinder (Fig. 2(b)), the current splits into a portion that flows beneath the cylinder, creating a jet-like flow, and another that flows over the cylinder. Eventually, the gravity current reestablishes itself downstream of the cylinder (Fig. 2(c)) and later on the quasisteady phase begins.

Simulations of currents without any obstacles using the configuration of Fig. 1 and the parameters of Table 1 with $H/h = 5$ were used to obtain time-averaged horizontal velocity profiles during the quasisteady state stage ($t/(h/V) = 8–12$) at the cylinder location ($x/h = 3$). The velocity profiles were found to resemble those of wall-jets, as found in Kneller et al. (1999), but with the velocity of the upper layer of light fluid directed upstream, and with a magnitude much less than that of the dense fluid (Simpson, 1997; p. 169). The calculated thickness of the boundary layer, taken here as the point where the horizontal velocity becomes 90% of its maximum, was found to be $\delta_{90}/h = 0.14$ and 0.08 for $\mathrm{Re} = 2000$ and 6000, respectively.

Table 1
Parameter values employed in the numerical simulations.

L/h	l/h	l_c/h	H/h	Re	Sc	D/h	G/h
24	9	3	5, 1	2000, 6000	1	0.15	0.01, 0.045, 0.1, 0.15, 0.2

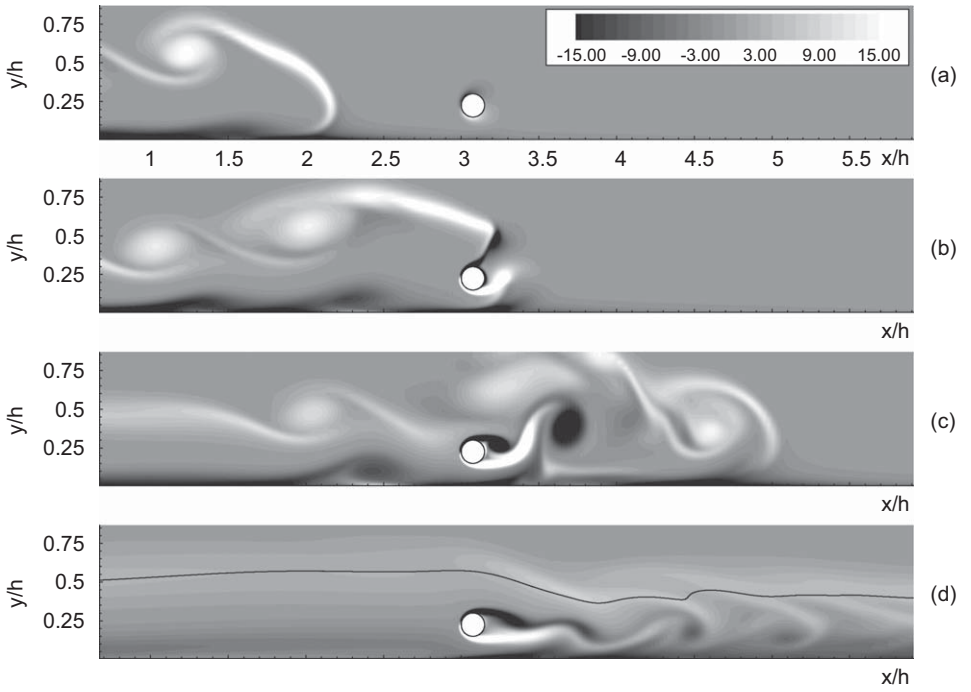

Fig. 2. Temporal evolution of the vorticity $\omega/(V/h)$ field as the gravity current interacts with the circular cylinder for $\mathrm{Re} = 2000$, $H/h = 5$, and $G/h = 0.15$: (a) $t/(h/V) = 2.36$, (b) $t/(h/V) = 3.4$, (c) $t/(h/V) = 5.3$, and (d) $t/(h/V) = 11.8$. The $c^* = 0.5$ concentration isoline is superimposed in (d).

3.3. Effect of the gap size

The force **F** exerted by the fluid on the cylinder was calculated by integrating the total pressure and the shear stress around the circumference of the cylinder (Panton, 1996; p. 385). Throughout the interaction of the current with the cylinder, the pressure contribution was found to be the dominant one. In order to eliminate any effect of p_{ref} on the temporal fluctuations of **F**, p_{ref} was evaluated at $x = L - l$ and $y = H/2$, where the velocity is negligible throughout the simulation. The x- and y-components of **F** are referred to as drag F_D and lift F_L, respectively. The drag and lift are scaled as $F_D/(0.5\rho_0 DV^2)$ and $F_L/(0.5\rho_0 DV^2)$, and time as $t/(h/V)$ (Gonzalez-Juez et al., 2008). This scaling is not used for the governing equations (1)–(3) because V is not known *a priori*.

Fig. 3 shows the variation of the drag and lift with time for various gaps (G/h) at $\mathrm{Re} = 2000$. As the current approaches the cylinder, the drag is seen to increase monotonically with time, until it reaches a first maximum by $t/(h/V) \approx 3.3$. The time of this first maximum defines the end of the impact stage, and the beginning of the transient stage of the interaction. The drag and lift fluctuate during the transient stage, and reach mean quasisteady values by $t/(h/V) \approx 8$, which represents the beginning of the quasisteady state stage.

3.3.1. Impact stage

The impact of the current on the cylinder has been observed to be essentially of two-dimensional nature (Gonzalez-Juez et al., 2008). Thus, two-dimensional simulations are expected to fully capture the dynamics during this stage. The dependence of the first drag maximum on G/h for $\mathrm{Re} = 2000$ and $H/h = 5$ is shown in Fig. 4(a). Note that the maximum drag decreases with increasing G/h. The same behavior was found for $\mathrm{Re} = 6000$, for gravity current flows past a square cylinder at $\mathrm{Re} = 2000$ (Gonzalez-Juez et al., 2007), and for experimental full-depth ($H/h = 1$) gravity current flows past a circular cylinder at $\mathrm{Re} \approx 10\,000$ (Ermanyuk and Gavrilov, 2005a). The reason for this decrease of the maximum drag with G/h lies in the decrease of the pressure acting on the upstream face of the cylinder as it is moved away from the wall. This pressure decrease can be observed in Fig. 5(a), where the instantaneous total pressure (viz. the combined dynamic and hydrostatic components of pressure) around the perimeter of the cylinder is shown for $G/h = 0.01$ and 0.15 at the time of maximum drag. Note from Fig. 5(a) that there is a low pressure region downstream and beneath the cylinder at $G/h = 0.15$. Thus, at small values of G/h the maximum drag results mainly from a high

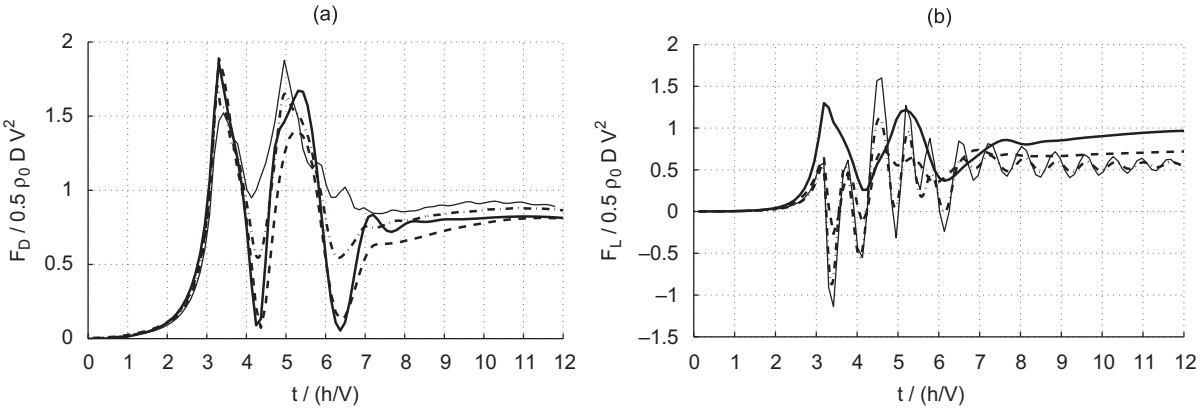

Fig. 3. Effect of G/h on the time-dependent drag (a) and lift (b) at $\mathrm{Re} = 2000$ and $H/h = 5$: $G/h = 0.01$ (thick solid line), 0.045 (dashed line), 0.1 (dash-dotted line), 0.15 (thin solid line). Notice in (b) the appearance of lift fluctuations for $t/(h/V) > 8$ when $G/h \geqslant 0.1$ ($G/D \geqslant 0.67$).

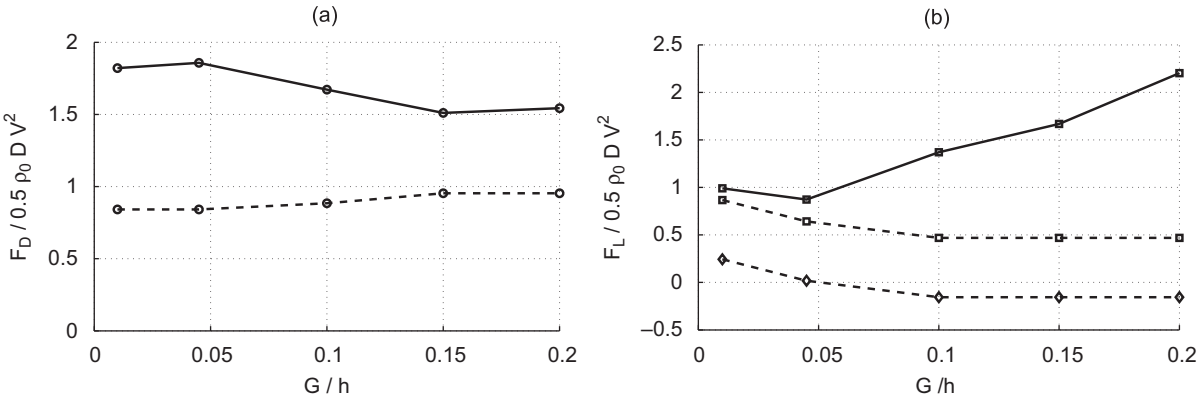

Fig. 4. Effect of G/h for $\mathrm{Re} = 2000$ and $H/h = 5$ on (a) the first drag maximum (solid line, circles) and the mean quasisteady state drag (dashed line, circles), and (b) on the magnitude of the initial lift fluctuation (solid line, squares), the mean quasisteady lift (dashed line, squares), and the mean quasisteady lift with the buoyant component subtracted (dashed line, diamonds).

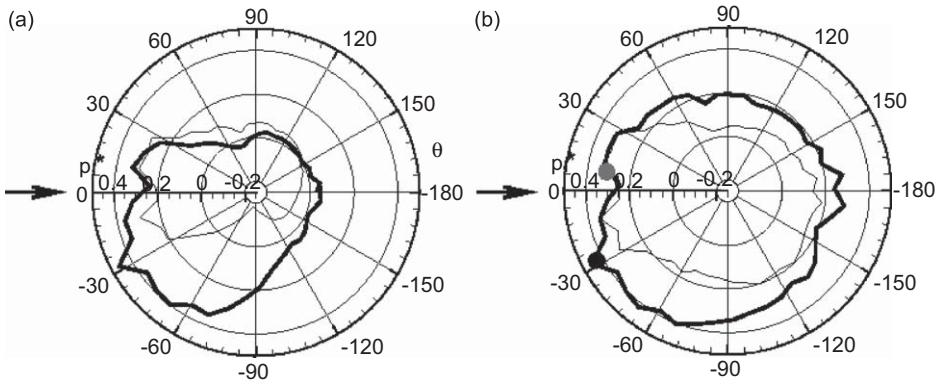

Fig. 5. Effect of G/h on the pressure distribution around the cylinder (a) at the time of maximum drag $t/(h/V) = 3.3$, and (b) during the quasisteady state stage $t/(h/V) \approx 8$–12 for $\mathrm{Re} = 2000$ and $H/h = 5$: $G/h = 0.01$ (thick solid line), 0.15 (thin solid line). The flow direction is shown. The stagnation points are indicated in (b) with large dots.

pressure region upstream of the cylinder, and at large values of G/h the maximum drag results, in addition, from a region of low pressure (suction) downstream and beneath the cylinder. Similar observations were made for the currents interacting with square cylinders (Gonzalez-Juez et al., 2007). The correlation of the maximum drag with G at different Re was not improved when making G dimensionless with δ_{90}, instead of with h.

Note in Fig. 3(b) that for $G/h \geqslant 0.045$ the lift first increases monotonically, and then decreases to a minimum by the end of the impact stage ($t/(h/V) \approx 3.3$). This initial lift fluctuation can reach a level of up to $F_L/0.5\rho_0 DV^2 \approx 2.5$, and is seen to increase with G/h, cf. Fig. 4(b). These results are consistent with experimental data for full-depth ($H/h = 1$) currents at $\mathrm{Re} \approx 10\,000$, which also show an increase of the initial lift fluctuation as the cylinder is moved away from the bottom wall (Ermanyuk and Gavrilov, 2005a). When the cylinder is moved towards the interface between the two fluids, and into the upper layer of light fluid, experiments show a decrease in the lift fluctuation. Such large values of G/h are not considered in the present work. The increase of the initial lift fluctuation with G/h occurs as more high-velocity dense fluid is allowed to flow beneath the cylinder when it is located farther away from the wall, cf. Fig. 2(b), leading to a larger decrease of the pressure beneath the cylinder, cf. case $G/h = 0.15$ of Fig. 5(a), and a more negative (directed downwards) minimum lift at $t/(h/V) \approx 3.3$. A further reason for this low pressure region at sufficiently large values of G/h is the formation of a counter-clockwise vortex beneath the cylinder, cf. Fig. 2(b). These two mechanisms were also observed for square cylinders (Gonzalez-Juez et al., 2007).

3.3.2. Transient stage

Fig. 3(a) shows that the magnitude of the initial drag fluctuation in the interval $t/(h/V) \approx 3.3$–5.4 can reach a level of up to $F_D/0.5\rho_0 DV^2 \approx 2$, and that it increases with decreasing G/h. As the cylinder is moved towards the wall, it is more exposed to the direct impact of vortical structures that form along the bottom wall, resulting in an increase of the initial drag fluctuation. The formation mechanism of these bottom wall vortical structures, which are detected even when a cylinder is absent, is attributed to flow separation induced by the Kelvin–Helmholtz vortices of the mixing layer (Gonzalez-Juez et al., 2008). The effect of these vortical structures on the drag variation with time at small values of G/h was found to be similar to previous observations for a bottom-mounted square cylinder (Gonzalez-Juez et al., 2008).

Regarding the lift, Fig. 3(b) shows persistent lift fluctuations throughout the transient stage ($3.3 < t/(h/V) < 8$), with a magnitude comparable to the initial lift fluctuation, and a frequency that scales with D. At $G/h = 0.15$, these lift fluctuations were seen to be enhanced by the temporary decrease of pressure induced near the cylinder by passing Kelvin–Helmholtz vortices, cf. Fig. 2(c). At $G/h = 0.045$, the enhancement was due to the decrease of pressure produced by vortical structures that are being convected along the bottom wall, and impinge on the cylinder.

The observations of the previous two paragraphs should be interpreted with care, however. Recently, two- and three-dimensional simulations of gravity current flows past bottom-mounted square and rectangular cylinders at $\mathrm{Re} \geqslant 7084$ have shown that Kelvin–Helmholtz vortices at the fluid interface, and vortical structures convected along the bottom wall, are unrealistically coherent and strong in two-dimensional simulations, leading to unphysical forces fluctuations (Gonzalez-Juez et al., 2008). Hence, we emphasize in this work the results for $\mathrm{Re} = 2000$. Efforts to assert the validity of the above observations with three-dimensional simulations are currently underway.

3.3.3. Quasisteady stage: force magnitude

The convection of Kelvin–Helmholtz vortices along the fluid interface, and of vortical structures along the bottom wall, and the associated enhancement of the force fluctuations were not observed after $t/(h/V) = 8$ for the parameters considered in this work, cf. Fig. 2(d) for example. Thus, our two-dimensional simulations should properly capture the forces on the cylinder during the quasisteady stage ($t/(h/V) > 8$). The most likely causes for damage to a submarine structure impacted by a gravity current are the large magnitude of the drag and lift fluctuation during impact, described in Section 3.3.1, and the *sustained* force fluctuations during the quasisteady stage, not the fluctuations of the forces during the transient stage. Therefore, in the following we focus on the quasisteady stage ($t/(h/V) > 8$).

We obtain quasisteady drag and lift values by averaging over the time interval $t/(h/V) = 8$–14. Since the supply of dense fluid is limited in the present lock-exchange configuration, the height and speed of the gravity current decrease beyond $t/(h/V) \approx 14$.

Fig. 4(a) shows that the quasisteady drag slightly increases with G/h, and has a value of approximately $F_D/0.5\rho_0 DV^2 = 0.9$. These findings correspond to observations for constant-density boundary layer flows past cylinders (Bearman and Zdravkovich, 1978; Lei et al., 1999; and others), for which the increase of the mean drag with G has been explained by a decreasing base pressure coefficient as the cylinder is moved away from the bottom wall (Lei et al., 1999). Furthermore, the cylinder is exposed to a more energetic free stream as it is moved out of the boundary layer. In comparison, a value of $F_D/0.5\rho_0 DV^2 \approx 1.3$ has been measured in the classic flow past a circular cylinder at about the same Re_D (Panton, 1996; p. 387).

The quasisteady lift displays quite interesting behavior. Fig. 4(b) shows that it decreases with G/h, and is directed upwards. In contrast to constant-density flows, gravity currents give rise to a buoyant component of the lift as the dense fluid engulfs the cylinder. This buoyant component of the lift can be estimated by taking the difference between the buoyant lift when the cylinder is immersed in light fluid, and that when it is immersed in dense fluid, cf. Fig. 2(d). This difference gives $F_{L,\mathrm{buo}}/0.5\rho_0 D u_b^2 = (\pi/2)(D/h)$. Fig. 4(b) shows the quasisteady lift with this buoyant component subtracted. Eliminating this buoyant component aids in identifying the other components of the lift.

It has been recognized in the study of constant-density flows past circular cylinders near walls that the mean lift is very sensitive to the location of the stagnation point (Lei et al., 1999). The location of the stagnation point was obtained in the present work by identifying the position on the cylinder where the streamline bifurcates. The large dots in Fig. 5(b) show the time-averaged locations of the stagnation points for $G/h = 0.01$ and 0.15 at $\mathrm{Re} = 2000$, as well as the total pressure distribution, time-averaged over the interval $t/(h/V) = 9$–12.5. Fig. 5(b) shows that the stagnation point is at -26° for $G/h = 0.01$, and at 7° for $G/h = 0.15$. These results are consistent with the positive (upwards) and negative (downward) values of the mean lift minus the buoyancy component shown in Fig. 4(b) for $G/h = 0.01$ and 0.15, respectively.

A combination of factors affects the position of the stagnation point. Firstly, as the gap decreases the stagnation point moves towards the wall (counter-clockwise), resulting in a positive component of the lift. This component dominates at small values of G/h. Secondly, the higher horizontal velocities found away from the wall because of the presence of a boundary layer, tend to move the stagnation point away from the wall (clockwise), resulting in a negative component of the lift. Both of these lift components are also found in the constant-density flow problem (Lei et al., 1999). As an interesting difference compared to constant-density flows, the mean lift minus the buoyancy component does not tend towards zero for large values of G/h, but instead approaches a negative value, cf. Fig. 4(b). Hence, there must be a third lift component, which appears to result from the constriction of the dense fluid flow downstream of the cylinder. Note in Fig. 2(d) the change of the dense fluid layer thickness at the cylinder location. This constriction tends to move the stagnation point away from the wall, and the wake towards the wall, as can be seen in Fig. 2(d) for $G/h = 0.15$, resulting in a negative lift component. This observation is supported by results, not shown here, from a simulation of a constant-density flow past a square cylinder in a plane channel, with the top wall curved in a way to simulate the interface between the two fluids in the gravity current flow. This third component of the lift is expected to decrease with D/h, as smaller cylinders distort the gravity current flow less.

3.3.4. *Quasisteady stage: onset of vortex shedding*

Because of the potential for resonant behavior, it is very important to know the conditions under which periodic lift fluctuations may appear due to vortex shedding or other mechanisms. The study of constant-density flows past circular cylinders near walls has shown that the occurrence of vortex shedding depends on G/D, Re_D, and the generation mechanism and velocity gradient of the boundary layer (Bearman and Zdravkovich, 1978; Zdravkovich, 1985; Lei et al., 1999, 2000). Fig. 3(b) shows that during the quasisteady state ($t/(h/V) > 8$) lift fluctuations appear when $G/h \geqslant 0.1$ for $\mathrm{Re} = 2000$ ($\mathrm{Re}_D = 177$), indicating the presence of a critical gap size in the range $(G/D)_{\mathrm{crit}} = 0.30$–0.67. These lift fluctuations are seen to have a dimensionless frequency of $\mathrm{St} \approx 0.2$, where the Strouhal number St is defined as $\mathrm{St} = f/(V/D)$, with f being the frequency of the lift fluctuations. The Strouhal number was calculated from a fairly short time interval of only 7–10 cycles, which nevertheless should suffice for the present discussion. The simulations show the lift fluctuations to be the result of the periodic shedding of vortices from the cylinder. These vortices downstream of the cylinder can be seen in Fig. 2(d) for $G/h = 0.15$, $\mathrm{Re} = 2000$, and $H/h = 5$. The simulations for $\mathrm{Re} = 6000$ ($\mathrm{Re}_D = 558$) confirmed the existence of a Strouhal number of approximately 0.2, and of a critical gap size in the range $(G/D)_{\mathrm{crit}} = 0.067$–0.3. This range for the critical gap size is consistent with results for constant-density flows, cf. Table 2, which shows data from the two-dimensional numerical simulations by Lei et al. (2000). In the

Table 2
Comparison of present simulation results with data from two-dimensional simulations of constant-density flows past circular cylinders near walls (Lei et al., 2000).

	Gravity current flow		Constant-density flow	
	$\mathrm{Re}_D = 177$	$\mathrm{Re}_D = 558$	$\mathrm{Re}_D = 200$	$\mathrm{Re}_D = 600$
$(G/D)_{\mathrm{crit}}$	0.30–0.67	0.067–0.3	0.6	0.3
$F_{L,\mathrm{rms}}/0.5\rho_0 D V^2$ at $G/D = 1$	–	0.55[a]	–	0.8

[a]It is 0.86 once a correction, discussed in the text, is made.

constant-density flow problem, the mechanism of vortex shedding suppression for small gaps is related to the cancellation of the vorticity in the cylinder's bottom shear layer by the vorticity of opposing sign in the bottom wall boundary layer (Taniguchi and Miyakoshi, 1990; Lei et al., 2000). The existence of this suppression mechanism was confirmed for the present gravity current flow problem.

3.4. Effect of the channel depth

There are two important effects of the ratio of the channel depth and the lock height (H/h) on the flowfield (Simpson, 1997). First, the horizontal velocities in the upper layer of light fluid are comparable to those in the bottom layer of dense fluid when $H/h = 1$, while the former velocities are much smaller than the latter when $H/h = 5$. Second, the gravity current front speed (V/u_b) is lower in currents with $H/h = 1$ ($V/u_b = 0.4$) than in currents with $H/h = 5$ ($V/u_b = 0.59$). Fig. 6 shows the effect of H/h on the lift variation with time for $\mathrm{Re} = 2000$ and $G/h = 0.15$. The mean quasisteady lift ($F_L/0.5\rho_0 DV^2$) with the buoyant component subtracted is -0.27 when $H/h = 1$ and -0.16 when $H/h = 5$. The more negative (directed downward) quasisteady lift in the $H/h = 1$ case is consistent with a stagnation point located slightly further away from the bottom wall (at 10°) in comparison with the $H/h = 5$ case (at 7°). Furthermore, this is consistent with a wake more directed towards the wall, as can be seen from a comparison of Figs. 2(d) and 7. More importantly, Fig. 6 shows that the decrease of H/h has eliminated the lift fluctuations for $\mathrm{Re} = 2000$ and $G/h = 0.15$. This was also observed for $\mathrm{Re} = 6000$. Notice also the absence of shed vortices during the quasisteady stage for $H/h = 1$ in Fig. 7, and their presence for $H/h = 5$ in Fig. 2(d). The lack of vortex shedding for $H/h = 1$ is confirmed by previous experimental measurements at $\mathrm{Re} \approx 10\,000$ (Ermanyuk and Gavrilov, 2005a). The cancellation of vortex shedding when $H/h = 1$ appears to result from the close proximity of the cylinder wake to the interface between thetwo fluids, which affects the potential shedding of vortices in two ways. First, notice that the layer of positive vorticity between the two fluids is more intense, and closer to the cylinder in the $H/h = 1$ case, cf. Figs. 2(d) and 7. Thus, if a vortex starts to shed from the top of the cylinder, its vorticity may be "cancelled" by that of opposing sign in the shear layer between the fluids. Second, the close proximity of the wake to the stratified layer between the fluids would suppress vertical velocity fluctuations, and the process of vortex shedding. There may be also an effect of the top wall, which is closer to the cylinder in the $H/h = 1$ case.

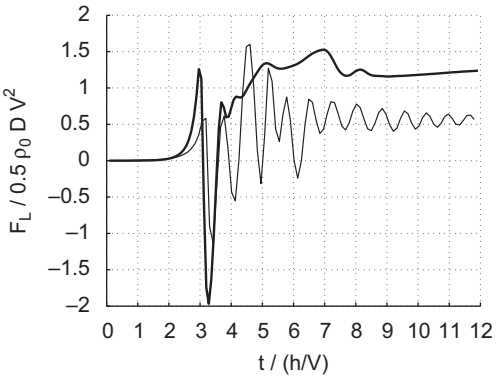

Fig. 6. Effect of H/h on the time-dependent lift for $\mathrm{Re} = 2000$ and $G/h = 0.15$: $H/h = 1$ (thick solid line), and $H/h = 5$ (thin solid line).

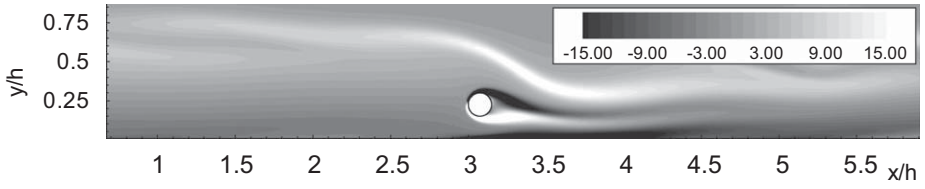

Fig. 7. Vorticity $\omega/(V/h)$ field as the gravity current interacts with the circular cylinder during the quasisteady stage ($t/(h/V) = 12$) for $\mathrm{Re} = 2000$, $H/h = 1$, and $G/h = 0.15$.

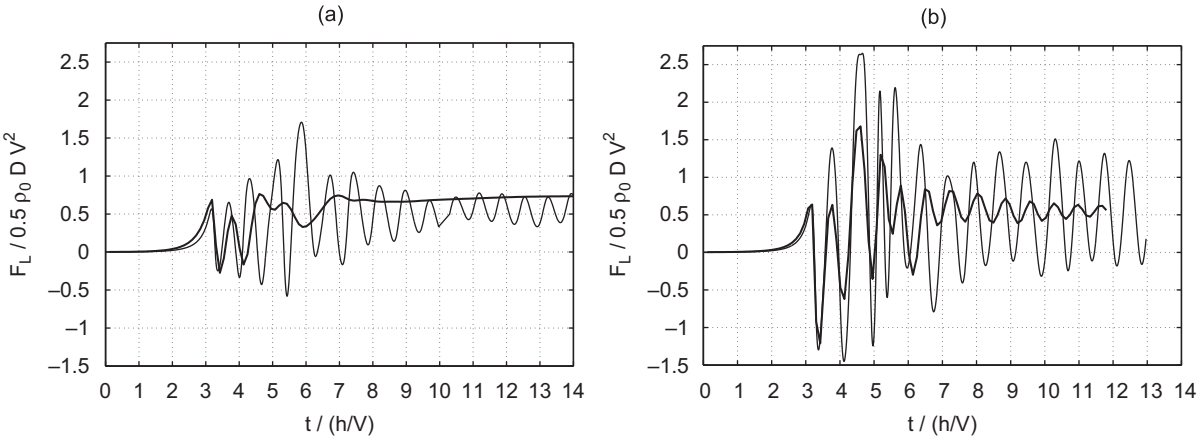

Fig. 8. Effect of Re (or Re_D) on the time-dependent lift for (a) $G/h = 0.045$ and (b) $G/h = 0.15$: $Re = 2000$ ($Re_D = 177$, thick solid line), and $Re = 6000$ ($Re_D = 558$, thin solid line). The lift fluctuations increase with Re (or Re_D) and with G/h.

3.5. Effect of the Reynolds number

An increase of Re from 2000 to 6000 was seen to have a small effect on the maximum drag and on the initial fluctuation of the lift during the impact stage ($t/(h/V) < 3.3$), cf. Fig. 8 for example. This is consistent with earlier observations for square cylinders (Gonzalez-Juez et al., 2007, 2008), in which Re is varied by an order of magnitude. For reasons discussed previously, we now focus on the quasisteady stage ($t/(h/V) > 8$). Fig. 8 shows the lift fluctuations to increase with Re (or Re_D) and with G/h during the quasisteady stage, consistent with observations for constant-density flows (Lei et al., 2000). The increase of the lift fluctuations when the cylinder is moved away from the bottom wall reflects the fact that the suppression of the vertical velocity fluctuations by the wall becomes less effective. The increase of these fluctuations with Re_D results from vortices being shed closer to the cylinder.

In the following, we focus on the case with $G/D = 1$ and $Re_D = 558$ in which the cylinder is sufficiently far away from the bottom wall for the lift fluctuations to almost reach their maximum level (Lei et al., 2000). Table 2 shows that the rms-fluctuations of the lift ($F_{L,\mathrm{rms}}/0.5\rho_0 DV^2$) found in the constant-density flow appear to be larger than those found in the present gravity current flow problem for $Re_D \approx 600$. Concerning this comparison, several issues need to be kept in mind. Firstly, the effect of different boundary layer thicknesses between the constant-density flow and the gravity current flow should be negligible since $G/\delta_{90} > 2$ for $Re_D \approx 600$. This implies that the cylinder sees the uniform stream in the constant-density flow and the almost uniform flow in the core of the gravity current. Secondly, the slightly larger value of Re_D in the constant-density flow is small enough to not have an important effect on the rms-fluctuations of the lift. Thirdly, the horizontal velocity of the uniform flow in the core of the current upstream of the cylinder is of about $0.8V$, instead of V. This horizontal velocity was calculated by taking time-averages during the quasi-steady state at different x-locations upstream of the obstacle. After correcting the rms-fluctuations of the lift by making them dimensionless with $0.8V$ instead of V we obtain a value of 0.86, which is very close to that found in the constant-density flow. Hence, the previous discussion suggests that a valid rough comparison of the rms-fluctuations of the lift between the constant-density flow past a circular cylinder and the flow considered here can be made, and that the magnitude of these fluctuations when the cylinder is sufficiently far away from the bottom wall is about the same in both types of flows. Similar conclusions were reached from the analysis of simulations at $Re = 10\,000$ and at $Re = 9000$ and $D/h = 0.1$.

4. Summary and conclusions

The present work investigates the flow of gravity currents past circular cylinders mounted above a wall, with an emphasis on the influence of the gap separating the cylinder from the wall. The dominant physical mechanisms generating the unsteady force are discussed, based on detailed information obtained from two-dimensional Navier–Stokes simulations.

The interaction can be divided into impact, transient, and quasisteady state stages. Because the impact has been observed to be essentially of two-dimensional nature (Gonzalez-Juez et al., 2008), our two-dimensional simulations fully capture the dynamics during this stage. During the impact stage, as the gravity current meets the cylinder, the drag increases monotonically towards a maximum, while the lift undergoes a drastic fluctuation. The gap is seen to have a small effect on the maximum drag during this stage, while its influence on the magnitude of the initial lift fluctuation is noticeable. This fluctuation increases with the gap size, as the velocity difference between the top and the bottom of the cylinder increases.

Unphysically large force fluctuations have been observed in two-dimensional simulations of gravity current flows past square cylinders (Gonzalez-Juez et al., 2008). For the parameters considered in the present work, such unphysical fluctuations were not observed during the quasisteady stage. During this stage, gravity current flows share several features with the well-studied constant-density boundary layer flows past circular cylinders near bottom walls. In both problems a critical gap size exists at which the forces begin to fluctuate as a result of vortex shedding. The fluctuations of the lift have a dimensionless frequency of about $St = 0.2$, their magnitude grows with Re and the gap size, and their magnitude is about the same to that found in constant-density flows for cylinders far away from the bottom wall. Furthermore, the wake vorticity interacts with the vorticity of the wall boundary layer, and for sufficiently small gap sizes this interaction can lead to the suppression of vortex shedding.

In spite of these common features, there are important differences between gravity current and constant-density flows. In the gravity current flow there is a component of the mean quasisteady lift due to buoyancy, and another component resulting from the constriction of dense fluid downstream of the cylinder which deflects the wake towards the wall. Among the different components of the mean quasisteady lift discussed, the buoyant component is the dominant one and, consequently, the mean quasisteady lift is directed upwards for all gap sizes. Another interesting difference is the effect of the ratio of the channel depth to lock height (H/h) in the gravity current flow: When this ratio is reduced from $H/h = 5$ to 1, the vortex shedding is cancelled for all gap sizes. The more intense shear layer between the two fluids when $H/h = 1$ seems to cancel the vorticity from vortices that start to shed from the top of the cylinder.

It is well known that gravity current fronts exhibit a pronounced spanwise structure related to the lobe-and-cleft instability (Simpson, 1997; Härtel et al., 2000a, b). The interaction of this instability mechanism with the spanwise modes for uniform flow past circular cylinders (Williamson, 1996) could give rise to novel dynamics that may significantly alter the force fields during the impact and transient stages. Furthermore, it will be of interest to explore how the current/structure interaction is modified by topographical features such as sloping bottom walls (Birman et al., 2007), and by non-Boussinesq effects of the gravity current (Birman et al., 2005). Finally, in the context of pipeline applications in the deep ocean, the present investigation should be extended to high Reynolds number turbidity currents (Necker et al., 2000, 2005), and include the effects of sediment deposition and erosion (Blanchette et al., 2005).

Acknowledgments

E.G.-J. is being supported by a National Science Foundation IGERT Grant DGE02-21715, as well as by a Cota-Robles fellowship. Computing time on a HP Opteron cluster has been provided by the California NanoSystems Institute at UC Santa-Barbara and Hewlett-Packard.

References

Bailey, S.C.C., Martinuzzi, R.J., Kopp, G.A., 2002. The effects of wall proximity on vortex shedding from a square cylinder: Three-dimensional effects. Physics of Fluids 14, 4160–4177.

Benjamin, T.B., 1968. Gravity currents and related phenomena. Journal of Fluid Mechanics 31, 209–248.

Bearman, P.W., Zdravkovich, M.M., 1978. Flow around a circular cylinder near a plane boundary. Journal of Fluid Mechanics 89, 33–47.

Birman, V.K., Martin, J.E., Meiburg, E., 2005. The non-Boussinesq lock-exchange problem. Part 2. High-resolution simulations. Journal of Fluid Mechanics 537, 125–144.

Birman, V.K., Battandier, B.A., Meiburg, E., Linden, P.F., 2007. Lock-exchange flows in sloping channels. Journal of Fluid Mechanics 577, 53–77.

Blanchette, F., Strauss, M., Meiburg, E., Kneller, B., Glinsky, M.E., 2005. High-resolution numerical simulations of resuspending gravity currents: Conditions for self-sustainment. Journal of Geophysical Research—Oceans 110.

Ermanyuk, E.V., Gavrilov, N.V., 2005a. Interaction of an internal gravity current with a submerged circular cylinder. Journal of Applied Mechanics and Technical Physics 46, 216–223.

Ermanyuk, E.V., Gavrilov, N.V., 2005b. Interaction of an internal gravity current with an obstacle on the channel bottom. Journal of Applied Mechanics and Technical Physics 46, 489–495.

Gonzalez-Juez, E.D., Constantinescu, S.G., Meiburg E., 2007. A study of the interaction of a gravity current with a square cylinder using two-dimensional numerical simulations. In: Proceedings of the 26th International Conference on Offshore Mechanics and Arctic Engineering OMAE2007-29280.

Gonzalez-Juez, E.D., Meiburg, E., Constantinescu, S.G., 2008. Gravity currents impinging on submerged cylinders: Flow fields and associated forces. Journal of Fluid Mechanics, accepted for publication.

Gonzalez-Juez, E.D., Meiburg, E., Constantinescu, S.G., 2009. Shallow water analysis of gravity current flows past isolated obstacles. Journal of Fluid Mechanics, submitted for publication.

Härtel, C., Meiburg, E., Necker, F., 2000a. Analysis and direct numerical simulation of the flow at a gravity-current head. Part 1. Flow topology and front speed for slip and no-slip boundaries. Journal of Fluid Mechanics 418, 189–212.

Härtel, C., Carlsson, F., Thunblom, M., 2000b. Analysis and direct numerical simulation of the flow at a gravity-current head. Part 2. The lobe-and-cleft instability. Journal of Fluid Mechanics 418, 213–229.

Kneller, B., Bennett, S.J., McCaffrey, W.D., 1999. Velocity structure, turbulence and fluid stresses in experimental gravity currents. Journal of Geophysical Research—Oceans 104, 5381–5391.

Lane-Serff, G.F., Beal, L.M., Hadfield, T.D., 1995. Gravity current flow over obstacles. Journal of Fluid Mechanics 292, 39–53.

Lei, C., Cheng, L., Armfield, S.W., Kavanagh, K., 2000. Vortex shedding suppression for flow over a circular cylinder near a plane boundary. Ocean Engineering 27, 1109–1127.

Lei, C., Cheng, L., Kavanagh, K., 1999. Re-examination of the effect of a plane boundary on force and vortex shedding of a circular cylinder. Journal of Wind Engineering and Industrial Aerodynamics 80, 263–286.

Liang, D.F., Cheng, L., 2005. Numerical model for wave-induced scour below a submarine pipeline. ASCE Journal of Waterway, Port, Coastal, and Ocean Engineering 131, 193–202.

Mittal, R., Balachandar, S., 1995. Effect of three-dimensionality on the lift and drag of nominally two-dimensional cylinders. Physics of Fluids 7, 1841–1865.

Necker, F., Hartel, C., Kleiser, L., Meiburg, E., 2000. High-resolution simulations of particle-driven gravity currents. International Journal of Multiphase Flow 28, 279–300.

Necker, F., Härtel, C., Kleiser, L., Meiburg, E., 2005. Mixing and dissipation in particle-driven gravity currents. Journal of Fluid Mechanics 545, 339–372.

Ooi, S.K., Constantinescu, S.G., Weber, L., 2005. Two-dimensional large eddy simulation of lock-exchange gravity current flows. In: Proceedings of the 31st International Association Hydraulic Research Congress.

Panton, R.L., 1996. Incompressible Flow. Wiley, New York.

Pierce, C.D., 2001. Progress-variable approach for large eddy simulation of turbulent combustion. Ph.D. Thesis, Stanford University.

Pierce, C.D., Moin, P., 2004. Progress-variable approach for large-eddy simulation of non-premixed turbulent combustion. Journal of Fluid Mechanics 504, 73–97.

Rottman, J.W., Simpson, J.E., Hunt, J.C.R., Britter, R.E., 1985. Unsteady gravity current flows over obstacles: some observations and analysis related to the phase II trials. Journal of Hazardous Materials 11, 325–340.

Shin, J.O., Dalziel, S.B., Linden, P.F., 2004. Gravity currents produced by lock exchange. Journal of Fluid Mechanics 521, 1–34.

Simpson, J.E., 1997. Gravity Currents in the Environment and the Laboratory. Cambridge University Press, Cambridge.

Sumer, B.M., Fredsoe, J., 1990. Scour below pipelines in waves. ASCE Journal of Waterway, Port, Coastal, and Ocean Engineering 116, 307–323.

Taniguchi, S., Miyakoshi, K., 1990. Fluctuating fluid forces acting on a circular cylinder and interference with a plane wall. Experiments in Fluids 9, 197–204.

Williamson, C.H.K., 1996. Vortex dynamics in the cylinder wake. Annual Review of Fluid Mechanics 28, 477–539.

Zdravkovich, M.M., 1985. Forces on a circular cylinder near a plane boundary. Applied Ocean Research 7, 197–201.